Temperature-dependent genetics of thermotolerance between yeast species

Melanie B. Abrams and Rachel B. Brem
Department of Plant and Microbial Biology, UC Berkeley, Berkeley, CA

ABSTRACT

Many traits of industrial and basic biological interest arose long ago, and manifest now as fixed differences between a focal species and its reproductively isolated relatives. In these systems, extant individuals can hold clues to the mechanisms by which phenotypes evolved in their ancestors. We harnessed yeast thermotolerance as a test case for such molecular-genetic inferences. In viability experiments, we showed that extant *Saccharomyces cerevisiae* survived at temperatures where cultures of its sister species *S. paradoxus* died out. Then, focusing on loci that contribute to this difference, we found that the genetic mechanisms of high-temperature growth changed with temperature. We also uncovered a robust signature of positive selection at thermotolerance loci in *S. cerevisiae* population sequences. We interpret these results in light of a model of gradual acquisition of thermotolerance in the *S. cerevisiae* lineage along a temperature cline. We propose that in an ancestral *S. cerevisiae* population, alleles conferring defects at a given temperature would have been resolved by adaptive mutations, expanding the range and setting the stage for further temperature advances. Together, our results and interpretation underscore the power of genetic approaches to explore how an ancient trait came to be.

INTRODUCTION

A central goal of evolutionary genetics is to understand how nature builds new phenotypes. Thanks to advances in statistical genetics and experimental evolution, mechanisms of trait evolution over relatively short timescales have come well within reach in the modern literature. By contrast, longer-term innovations have posed a more profound challenge for the field (Orr 2001). In principle, for a phenotype that originated long ago and manifests now as a fixed difference between species, evolution could have refined the character along the entire divergence time of the respective taxa. In landmark cases, candidate-gene studies have shed light on suites of mutational changes of this kind between species, at a given model locus. This includes the order by which adaptive alleles were likely acquired, and/or the functional pressures that drove them (Bridgham et al. 2009; Baldwin et al. 2014; Dong et al. 2014; Sayou et al. 2014; Anderson et al. 2015; Daugherty et al. 2016; Sulak et al. 2016; Liu et al. 2018; Starr et al. 2018; Xie et al. 2018; Siddiq and Thornton 2019; Pillai et al. 2020; Prieto-Godino et al. 2021). But, in most cases, any factor pursued by such a candidate-gene approach only represents part of the complex genetic architecture of an ancient trait. We still know relatively little about how evolution coordinates multiple adaptive loci over deep divergences.

In the search for evolutionary principles, genetically tractable model systems can be of great utility. *Saccharomyces* yeasts are well suited for this purpose, and environmental yeast isolates have been studied extensively for their innovations within and between species (Hittinger 2013). Thermotolerance is of particular interest because it tracks with phylogeny across the 20 million years of the *Saccharomyces* radiation (Gonçalves et al. 2011; Salvadó et al. 2011). Even the two most recent branches of the phylogeny exhibit

a robust difference in this phenotype: *S. cerevisiae* acquired the ability to grow at temperatures near 40°C in the five million years since it diverged from its sister species, *S. paradoxus* (Sweeney et al. 2004; Gonçalves et al. 2011; Salvadó et al. 2011; Williams et al. 2015). Previously, a whole-genome mapping scheme was used to identify housekeeping genes at which variation between *S. cerevisiae* and *S. paradoxus* impacts growth at the high end of the *S. cerevisiae* temperature range (Weiss et al. 2018). These loci exhibit striking sequence differences between the species, and conservation in *S. cerevisiae*, consistent with a history of positive selection on pro-thermotolerance alleles (Weiss et al. 2018; Abrams et al. 2021a,b). However, we have as yet little insight into the ecological dynamics by which this model trait evolved along the *S. cerevisiae* lineage.

Cases of adaptation across temperature clines are a mainstay of the evolutionary genetics literature (Turner et al. 2008; Prasad et al. 2011; Mimura et al. 2013; Savolainen et al. 2013; Robin et al. 2017; Dudaniec et al. 2018; Key et al. 2018; Endler 2020; Tepolt and Palumbi 2020; Calfee et al. 2021; Machado et al. 2021). Here we sought to explore the relevance of such a mechanism to the events by which *S. cerevisiae* gained its maximal thermotolerance phenotype. Given that we have no access to genotypes representing ancient intermediates between this species and *S. paradoxus*, we designed a strategy to interrogate the genetics of extant strains, focusing on contributing genes of major effect. We surveyed gene-environment interactions by these thermotolerance loci across warm temperatures, complementing previous studies of interspecies variation at a single high temperature (Weiss et al. 2018; Abrams et al. 2021b). And we assessed the evidence for selective sweeps at these loci with a population-genomic approach.

RESULTS

For an initial study of the genetics of yeast species variation in temperature response, we chose to harness DVBPG1373, an *S. cerevisiae* isolate from Dutch soil, and Z1, an *S. paradoxus* isolate from an oak tree in England. We anticipated that detailed analyses using these strains, as representatives of their respective species, could accelerate the discovery of more general principles (Weiss et al. 2018; Abrams et al. 2021a,b). We developed an assay quantifying cell viability in a given liquid culture before and after incubation at a temperature of interest, and we implemented this approach for each species in turn. The results revealed an advantage for *S. cerevisiae* over *S. paradoxus* at temperatures above 35°C (Figure 1), consistent with previous growth-based surveys (Sweeney et al. 2004; Gonçalves et al. 2011; Salvadó et al. 2011; Williams et al. 2015). *S. cerevisiae* maintained viability at all temperatures tested, whereas by 37°C, *S. paradoxus* became inviable, with no evidence for spontaneous rescue even over long incubation times (Figure 1). Using the latter as a window onto the phenotype of the common ancestor of *S. cerevisiae* and *S. paradoxus*, we would envision that this ancient population would have gone extinct rather than adapting, if exposed to temperatures at the high end of the range tolerated by modern *S. cerevisiae*.

We next aimed to investigate the genetics of temperature response as it differs between extant *S. cerevisiae* and *S. paradoxus,* to motivate inferences about the evolution of the maximal thermotolerance trait. We focused on four genes—the cell division factors *ESP1, MYO1,* and *CEP3*, and the ribosome maturation factor *AFG2*—where alleles from modern *S. paradoxus* compromise growth at 39°C (Weiss et al. 2018). We made use of strains of the *S. cerevisiae* DVBPG1373 background harboring the allele of each gene in turn from *S. paradoxus* Z1. In each, we measured the growth phenotype as a dose-response across temperatures, and observed a drop as temperature increased (Figure 2). In the *S. cerevisiae* background, *S. paradoxus* Z1 alleles eroded growth efficiency at temperatures well below the hard limit of viability for the Z1 wild-type (~38°C), an effect that reached significance for three of our four focal genes (Figure 2). We conclude that many problems posed by *S. paradoxus* Z1 alleles at the high end of our temperature range also manifest to a lesser extent at lower temperatures.

Inspecting the shape of the temperature dose-responses of allelic effects, we noted quantitative differences between our loci. At the chromatid separase gene *ESP1*, the Z1 allele conferred an appreciable drop in growth efficiency at 36°C and supported almost no growth by 37°C (Figure 2B). By contrast, at *AFG2,* the *S. paradoxus* Z1 allele was sufficient for growth approximating that of *S. cerevisiae* until 38°C (Figure 2D). The dose-response of allelic effects at *MYO1,* encoding a class II myosin heavy chain, lay between these two extremes (Figure 2C). This differential susceptibility to temperature across the genes of our set likely reflects distinguishing properties of their structure and function, and of the interspecies variants they harbor.

We reasoned that trends from our temperature dose-response approach would be most informative when they were conserved across *S. paradoxus* as a species. To pursue this, we earmarked *ESP1*, whose *S. paradoxus* Z1 allele had exhibited the sharpest falloff with temperature among the genes of our set (Figure 2B). We repeated our growth efficiency experiments in strains of *S. cerevisiae* DVBPG1373 harboring *ESP1* from other *S. paradoxus* donors beside the Z1 strain. These transgenics, which phenocopy wild-type DVBPG1373 at 28°C (Weiss et al. 2018), all dropped off in growth efficiency by 36°C (Figure S2), as expected if the temperature preference of *ESP1* were ancestral to, and shared across, extant *S. paradoxus* populations.

Together, these dose-response results make clear that the functions of *S. paradoxus* alleles at our focal genes break down at distinct temperatures between 35°C and 38°C—suggesting similar gene-by-environment effects in the ancestor of *S. cerevisiae* and *S. paradoxus*, if it sampled a range of temperature conditions over evolutionary history.

To gain insight into past and current selective pressures on thermotolerance loci, we turned to a molecular-evolution approach. Previous work on *Saccharomyces* thermotolerance genes has emphasized sequence divergence between species (Weiss et al. 2018; Abrams et al. 2021a,b). For a complementary focus on population variation within *S. cerevisiae*, we analyzed the Tajima's D statistic, which formulates properties of sequence variants in a population into a selection test on allele frequencies (Tajima

1989; Biswas and Akey 2006). We first developed a resampling-based test that compares Tajima's D between a gene cohort of interest and a genomic null. This scheme enables a non-parametric assessment of significance and normalizes out potential effects of demography (see Methods). Expecting that our test would have maximal power in a data set of large sample size, we focused on the most deeply-sampled *S. cerevisiae* population in current compendia, comprising isolates from vineyards and European soil (Peter et al. 2018). Examining our four focal thermotolerance genes, we detected an enrichment for negative Tajima's D at these loci across *S. cerevisiae* genomes, reporting an excess of rare variants—a classic signature of a selective sweep (Figure 3 and Table S1). We repeated this analysis using more comprehensive sets of hits from interspecies thermotolerance screens (Weiss et al. 2018; Abrams et al. 2021a,b), and detected strong signal for negative Tajima's D at these loci in vineyard/European *S. cerevisiae* in every case (Table S1). Interestingly, *ESP1* exhibited the most negative Tajima's D value among all thermotolerance genes (Table S1), dovetailing with the strong effect of variation at this gene in phenotypic analyses (Weiss et al. 2018 and Figure 2). The trend for low Tajima's D in thermotolerance genes was detectable but not consistent across other shallowly-sampled populations of *S. cerevisiae* (see Methods), potentially reflecting weaker power or weaker selection in the latter relative to vineyard/European strains. In either case, our data establish that thermotolerance gene variation in some modern *S. cerevisiae* populations follows the expectations after a past sweep, with relatively few recent mutations popping up on an otherwise constrained adaptive haplotype.

DISCUSSION

Most trait differences that define long-diverged species are likely the product of suites of unlinked variants that have come together over long timescales. Tracing the ancient evolutionary events at such loci remains a central challenge in the field. In this work, we have characterized thermotolerance genes in extant yeast strains and species to inform models of the evolution of the trait in *S. cerevisiae*.

Our data have shown that temperatures below the high end of the *S. cerevisiae* range are lethal for *S. paradoxus*. This complements previous surveys of the *Saccharomyces* clade using growth-based assays (Sweeney et al. 2004; Gonçalves et al. 2011; Salvadó et al. 2011) and reveals that, under high temperature conditions, a given culture of *S. paradoxus* will die off rather than adapting. Assuming similar behavior in an ancestor of *S. cerevisiae* before the rise of its modern thermotolerance profile, we infer that the latter event was unlikely to be precipitated by a single jump to a hot growth environment, long ago in history. Rather, we favor the hypothesis that thermotolerance evolution through the *S. cerevisiae* lineage proceeded along a temperature cline, as has been documented in elegant local-adaptation case studies (Mimura et al. 2013; Robin et al. 2017; Dudaniec et al. 2018; Key et al. 2018; Tepolt and Palumbi 2020). In this scenario, a well-adapted ancestral *S. cerevisiae* population in a given temperature niche would have acquired variants that resolved defects manifesting in slightly warmer conditions, and expanded its range. If the *S. cerevisiae* lineage did go through a series of such transitions in acquiring maximal thermotolerance, it would echo the principle that

188 gradual exposure to increasing stresses fosters adaptation and reduces the risk of
189 extinction, relative to a sudden, high dose of stress (Lindsey et al. 2013).
190
191 We have also leveraged results from genetic mapping of *S. cerevisiae* thermotolerance
192 to trace the temperature dependence of contributing genes. This contrasts with
193 approaches that search genomes for variants associated with environment or
194 population variables (Rellstab et al. 2015; Hoban et al. 2016), in that we focus directly
195 on *bona fide* causal determinants of the trait of interest. Our strategy has allowed us to
196 discern differences between thermotolerance loci in terms of the temperatures at which
197 alleles from modern *S. paradoxus* fail in their growth functions. In other words, the
198 genetic mechanisms of viability change with temperature in this system. If such effects
199 were at play in the *S. cerevisiae* ancestor, as it sampled conditions and niches during
200 the acquisition of thermotolerance, each locus would have come under selective
201 pressure at the temperature where its defect manifested. This phenomenon, by which
202 the weakest point in the genetic network targeted by evolution changes as conditions
203 change, has been termed “whack-a-mole” dynamics (Shin and MacCarthy 2015).
204 Ultimately, a complete model of adaptation across time and environment will take into
205 account the shifts in the evolutionary landscape from this effect as well as from constant
206 changes in genetic background (Starr and Thornton 2016).
207
208 If the ancient *S. cerevisiae* population did adapt progressively along a temperature
209 cline, what would the ecology have been? In principle, migrants from temperate physical
210 locales could have advanced to warmer and warmer locales, perhaps terminating in the
211 hot East Asian environments to which the ancestor of modern *S. cerevisiae* has been
212 traced (Peter et al. 2018). Alternatively, the trait syndrome in this species—a unique
213 ability to tolerate ethanol as well as heat, with both given off by fermentative
214 metabolism—could have arisen as a specialization to kill off microbial competitors in
215 nutrient-rich substrates, regardless of the endemic temperature of the location (Goddard
216 2008; Salvadó et al. 2011). If so, variants would have been acquired, potentially over
217 millions of generations, gradually to ratchet up fermentative activity and tolerance to its
218 byproducts, with our genetic insights thus far largely restricted to the latter.
219
220 Our work also leaves open the dating of any such events. In several *S. cerevisiae*
221 populations, we have uncovered patterns of allele frequency at thermotolerance loci
222 consistent with a history of positive selection. Previous work across populations has
223 also made clear that *S. cerevisiae* alleles at our focal genes are partly sufficient for
224 maximal thermotolerance, conserved within the species, and divergent from *S.*
225 *paradoxus* (Weiss et al. 2018; Abrams et al. 2021b). We thus propose that many of
226 these alleles were acquired in ancient selective sweeps, before the radiation of modern
227 *S. cerevisiae*. That said, later refinements in particular populations of *S. cerevisiae* may
228 also have strengthened beneficial facets of the trait, added regulatory tuning, or
229 eliminated antagonistic pleiotropic “side effects” that were niche-specific. A
230 comprehensive genetic and ecological reconstruction of this history may be out of our
231 current grasp, especially in light of the caveats of our approach using a laboratory
232 setting and extant strain backgrounds. Nonetheless, our data add compelling detail to

233 an emerging consensus view of how evolution built maximal thermotolerance in *S.*
234 *cerevisiae*.
235
236 **METHODS**
237
238 **Dose response growth assay**
239
240 For growth measurements in Figure 2, we assayed *S. paradoxus* Z1, *S. cerevisiae*
241 DBVPG1373, and *S. cerevisiae* DBVPG1373 with the *S. paradoxus* Z1 allele of *ESP1*,
242 *MYO1, AFG2,* or *CEP3* swapped in at the endogenous locus from (Weiss et al. 2018)
243 (Table S2) as follows. Each strain was streaked from a -80°C freezer stock onto a yeast
244 peptone dextrose (YPD) agar plate and incubated at room temperature for 3 days. For
245 each biological replicate, a single colony was inoculated into 5 mL liquid YPD and
246 grown for 24 hours at 28°C with shaking at 200 rpm to generate pre-cultures. Each pre-
247 culture was backdiluted into YPD at an OD_{600}/mL of 0.05 and grown for an additional
248 5.5-6 hours at 28°C, shaking at 200 rpm, until reaching logarithmic phase. Each pre-
249 culture was again back-diluted into 10 mL YPD in 1-inch diameter glass tubes with a
250 target OD_{600}/mL of 0.05; the actual OD_{600}/mL of each was measured, after which it was
251 grown at a temperature of interest (28°C or 35-38°C) with shaking at 200rpm for 24
252 hours, and OD_{600}/mL was measured again. The growth efficiency for each replicate was
253 calculated as the difference between these final and initial OD_{600}/mL values. We used
254 the growth efficiency from all days and all temperatures of a given strain *s* as input into
255 a two-factor type 2 ANOVA test for a temperature-by-strain effect comparing *s* with *S.*
256 *cerevisiae*.
257
258 For growth measurements of *ESP1* swap strains with different donors, as reported in
259 Figure S2, cultures were grown and measured as above, except that the only
260 temperature was 36°C.
261
262 **Viability assay**
263
264 For the survey of viability phenotypes at high temperatures across wild-type isolates in
265 Figure 2, strains were streaked out and a colony of each was pre-cultured in liquid as
266 for 39°C growth above, except that the initial pre-culture to achieve saturation lasted 48
267 hours. Each pre-culture was back-diluted into 10 mL of YPD to reach an OD600/mL of
268 0.05 and then cultured for 24 hours at the temperature of interest (28°C - 39°C). The
269 viability of both the precultures and the cultures after 24 hours at the temperature of
270 interest were measured with a spotting assay, where we diluted aliquots from the
271 culture in a 1:10 series and spotting 3 µL of each dilution for growth on a solid YPD
272 plate. After incubation at 28°C for two days, we used the dilution corresponding to the
273 densest spot that was not a lawn for to determine viability: we counted the number of
274 colonies in each of the two technical replicate spots, formulated the number of colony
275 forming units per mL of undiluted culture (CFU/mL). We determined the change in
276 viable cells by subtracting the number of cells in the culture at the initial time point from
277 that at the final timepoint, based on the CFU/mL count and the culture volume. We

evaluated the significance of the difference between *S. cerevisiae* and *S. paradoxus* at a given temperature using a one-sided Mann-Whitney U test.

Tajima's D in Wine/European *S. cerevisiae*

Tajima's D tabulates the difference between the average number of differences in pairs of sequences in a population sample and the number of variant sites in the sample. When the latter is of much bigger magnitude and D is negative, it indicates that variation in the sample is accounted for mostly by rare alleles, as expected some time after a selective sweep when *de novo* mutations arise on the swept haplotype. Taking as input the VCFs reporting inheritance in the strains of a given *S. cerevisiae* population from (Peter et al. 2018), we used VCF-kit (Cook and Andersen 2017) to calculate Tajima's D for the region from coding start to coding stop for each gene. We then sampled 10,000 random cohorts of genes from the genome with the same number of essential and nonessential genes as our thermotolerance cohort (Winzeler et al. 1999), and we used as an empirical *P*-value the proportion of random cohorts where the median Tajima's D was less than or equal to that of our thermotolerance cohort. Application of this test to the Wine/European *S. cerevisiae* population (362 strains) is reported in Figure 3 of the main text. Applied to the Mosaic Region 3 (113 strains), Mixed Origin (72 strains), Sake (47 strains), and Brazilian Bioethanol (35 strains), the four next most deeply sampled populations from (Peter et al. 2018), this test for enrichment of low Tajima's D among our four focal thermotolerance genes yielded $P = 0.8351$, 0.975, 0.8624, and 0.0348 respectively.

CONFLICT OF INTEREST

The authors have declared no conflict of interest.

ACKNOWLEDGEMENTS

This work was supported by NSF GRFP DGE 1752814 to M.A. and NIH R01 GM120430 to R.B.B. The authors thank Faisal AlZaben, Abel Duarte, and Jude Edwards for experimental support and Adam Arkin for his generosity with computational resources.

LITERATURE CITED

Abrams, M. B., J. N. Chuong, F. AlZaben, C. A. Dubin, J. M. Skerker, and R. B. Brem. 2021a. Barcoded reciprocal hemizygosity analysis via sequencing illuminates the complex genetic basis of yeast thermotolerance.

Abrams, M. B., C. A. Dubin, F. AlZaben, J. Bravo, P. M. Joubert, C. V. Weiss, and R. B. Brem. 2021b. Population and comparative genetics of thermotolerance divergence between yeast species. G3 Genes|Genomes|Genetics, doi: https://doi.org/10.1093/g3journal/jkab139.

Anderson, D. W., A. N. McKeown, and J. W. Thornton. 2015. Intermolecular epistasis shaped the function and evolution of an ancient transcription factor and its DNA binding sites. eLife 4:e07864.

Baldwin, M. W., Y. Toda, T. Nakagita, M. J. O'Connell, K. C. Klasing, T. Misaka, S. V. Edwards, and S. D. Liberles. 2014. Sensory biology. Evolution of sweet taste perception in hummingbirds by transformation of the ancestral umami receptor. Science 345:929–933.

Biswas, S., and J. M. Akey. 2006. Genomic insights into positive selection. Trends in Genetics 22:437–446.

Bridgham, J. T., E. A. Ortlund, and J. W. Thornton. 2009. An epistatic ratchet constrains the direction of glucocorticoid receptor evolution. Nature 461:515–519.

Calfee, E., D. Gates, A. Lorant, M. T. Perkins, G. Coop, and J. Ross-Ibarra. 2021. Selective sorting of ancestral introgression in maize and teosinte along an elevational cline. PLOS Genetics 17:e1009810. Public Library of Science.

Cook, D. E., and E. C. Andersen. 2017. VCF-kit: assorted utilities for the variant call format. Bioinformatics 33:1581–1582.

Daugherty, M. D., A. M. Schaller, A. P. Geballe, and H. S. Malik. 2016. Evolution-guided functional analyses reveal diverse antiviral specificities encoded by IFIT1 genes in mammals. eLife 5:e14228.

Dong, S., R. Stam, L. M. Cano, J. Song, J. Sklenar, K. Yoshida, T. O. Bozkurt, R. Oliva, Z. Liu, M. Tian, J. Win, M. J. Banfield, A. M. E. Jones, R. A. L. van der Hoorn, and S. Kamoun. 2014. Effector specialization in a lineage of the Irish potato famine pathogen. Science 343:552–555.

Dudaniec, R. Y., C. J. Yong, L. T. Lancaster, E. I. Svensson, and B. Hansson. 2018. Signatures of local adaptation along environmental gradients in a range-expanding damselfly (Ischnura elegans). Molecular Ecology 27:2576–2593.

348 Endler, J. A. 2020. Geographic Variation, Speciation and Clines. (MPB-10), Volume 10.
349 Princeton University Press.
350 Goddard, M. R. 2008. Quantifying the complexities of Saccharomyces cerevisiae's
351 ecosystem engineering via fermentation. Ecology 89:2077–2082.
352 Gonçalves, P., E. Valério, C. Correia, J. M. G. C. F. de Almeida, and J. P. Sampaio.
353 2011. Evidence for Divergent Evolution of Growth Temperature Preference in
354 Sympatric Saccharomyces Species. PLOS ONE 6:e20739.
355 Hittinger, C. T. 2013. Saccharomyces diversity and evolution: a budding model genus.
356 Trends Genet 29:309–317.
357 Hoban, S., J. L. Kelley, K. E. Lotterhos, M. F. Antolin, G. Bradburd, D. B. Lowry, M. L.
358 Poss, L. K. Reed, A. Storfer, and M. C. Whitlock. 2016. Finding the Genomic
359 Basis of Local Adaptation: Pitfalls, Practical Solutions, and Future Directions. Am
360 Nat 188:379–397.
361 Key, F. M., M. A. Abdul-Aziz, R. Mundry, B. M. Peter, A. Sekar, M. D'Amato, M. Y.
362 Dennis, J. M. Schmidt, and A. M. Andrés. 2018. Human local adaptation of the
363 TRPM8 cold receptor along a latitudinal cline. PLOS Genetics 14:e1007298.
364 Public Library of Science.
365 Lindsey, H. A., J. Gallie, S. Taylor, and B. Kerr. 2013. Evolutionary rescue from
366 extinction is contingent on a lower rate of environmental change. Nature
367 494:463–467.
368 Liu, Q., P. Onal, R. R. Datta, J. M. Rogers, U. Schmidt-Ott, M. L. Bulyk, S. Small, and J.
369 W. Thornton. 2018. Ancient mechanisms for the evolution of the bicoid
370 homeodomain's function in fly development. Elife 7.
371 Machado, H. E., A. O. Bergland, R. Taylor, S. Tilk, E. Behrman, K. Dyer, D. K. Fabian,
372 T. Flatt, J. González, T. L. Karasov, B. Kim, I. Kozeretska, B. P. Lazzaro, T. J.
373 Merritt, J. E. Pool, K. O'Brien, S. Rajpurohit, P. R. Roy, S. W. Schaeffer, S.
374 Serga, P. Schmidt, and D. A. Petrov. 2021. Broad geographic sampling reveals
375 the shared basis and environmental correlates of seasonal adaptation in
376 Drosophila. eLife 10:e67577. eLife Sciences Publications, Ltd.
377 Mimura, M., K. Ono, K. Goka, and T. Hara. 2013. Standing variation boosted by multiple
378 sources of introduction contributes to the success of the introduced species,
379 Lotus corniculatus. Biol Invasions 15:2743–2754.
380 Orr, H. A. 2001. The genetics of species differences. Trends Ecol Evol 16:343–350.
381 Peter, J., M. D. Chiara, A. Friedrich, J.-X. Yue, D. Pflieger, A. Bergström, A. Sigwalt, B.
382 Barre, K. Freel, A. Llored, C. Cruaud, K. Labadie, J.-M. Aury, B. Istace, K.
383 Lebrigand, P. Barbry, S. Engelen, A. Lemainque, P. Wincker, G. Liti, and J.
384 Schacherer. 2018. Genome evolution across 1,011 Saccharomyces cerevisiae
385 isolates. Nature 556:339–344.
386 Pillai, A. S., S. A. Chandler, Y. Liu, A. V. Signore, C. R. Cortez-Romero, J. L. P.
387 Benesch, A. Laganowsky, J. F. Storz, G. K. A. Hochberg, and J. W. Thornton.
388 2020. Origin of complexity in haemoglobin evolution. Nature 581:480–485.
389 Prasad, A., M. J. F. Croydon-Sugarman, R. L. Murray, and A. D. Cutter. 2011.
390 Temperature-Dependent Fecundity Associates with Latitude in Caenorhabditis
391 Briggsae. Evolution 65:52–63.

392 Prieto-Godino, L. L., H. R. Schmidt, and R. Benton. 2021. Molecular reconstruction of
393 recurrent evolutionary switching in olfactory receptor specificity. eLife 10:e69732.
394 eLife Sciences Publications, Ltd.
395 Rellstab, C., F. Gugerli, A. J. Eckert, A. M. Hancock, and R. Holderegger. 2015. A
396 practical guide to environmental association analysis in landscape genomics. Mol
397 Ecol 24:4348–4370.
398 Robin, C., A. Andanson, G. Saint-Jean, O. Fabreguettes, and C. Dutech. 2017. What
399 was old is new again: thermal adaptation within clonal lineages during range
400 expansion in a fungal pathogen. Molecular Ecology 26:1952–1963.
401 Salvadó, Z., F. N. Arroyo-López, J. M. Guillamón, G. Salazar, A. Querol, and E. Barrio.
402 2011. Temperature adaptation markedly determines evolution within the genus
403 Saccharomyces. Appl Environ Microbiol 77:2292–2302.
404 Savolainen, O., M. Lascoux, and J. Merilä. 2013. Ecological genomics of local
405 adaptation. Nature Reviews Genetics 14:807–820.
406 Sayou, C., M. Monniaux, M. H. Nanao, E. Moyroud, S. F. Brockington, E. Thévenon, H.
407 Chahtane, N. Warthmann, M. Melkonian, Y. Zhang, G. K.-S. Wong, D. Weigel, F.
408 Parcy, and R. Dumas. 2014. A Promiscuous Intermediate Underlies the Evolution
409 of LEAFY DNA Binding Specificity. Science 343:645–648. American Association
410 for the Advancement of Science.
411 Shin, J., and T. MacCarthy. 2015. Antagonistic Coevolution Drives Whack-a-Mole
412 Sensitivity in Gene Regulatory Networks. PLoS Comput Biol 11:e1004432.
413 Siddiq, M. A., and J. W. Thornton. 2019. Fitness effects but no temperature-mediated
414 balancing selection at the polymorphic Adh gene of Drosophila melanogaster.
415 PNAS 116:21634–21640. National Academy of Sciences.
416 Starr, T. N., J. M. Flynn, P. Mishra, D. N. A. Bolon, and J. W. Thornton. 2018. Pervasive
417 contingency and entrenchment in a billion years of Hsp90 evolution. PNAS
418 115:4453–4458. National Academy of Sciences.
419 Starr, T. N., and J. W. Thornton. 2016. Epistasis in protein evolution. Protein Science
420 25:1204–1218.
421 Sulak, M., L. Fong, K. Mika, S. Chigurupati, L. Yon, N. P. Mongan, R. D. Emes, and V.
422 J. Lynch. 2016. TP53 copy number expansion is associated with the evolution of
423 increased body size and an enhanced DNA damage response in elephants. eLife
424 5:e11994.
425 Sweeney, J. Y., H. A. Kuehne, and P. D. Sniegowski. 2004. Sympatric natural
426 Saccharomyces cerevisiae and S. paradoxus populations have different thermal
427 growth profiles. FEMS Yeast Res. 4:521–525.
428 Tajima, F. 1989. Statistical Method for Testing the Neutral Mutation Hypothesis by DNA
429 Polymorphism. Genetics 123:585–595.
430 Tepolt, C. K., and S. R. Palumbi. 2020. Rapid Adaptation to Temperature via a Potential
431 Genomic Island of Divergence in the Invasive Green Crab, Carcinus maenas.
432 Frontiers in Ecology and Evolution 8:411.
433 Turner, T. L., M. T. Levine, M. L. Eckert, and D. J. Begun. 2008. Genomic Analysis of
434 Adaptive Differentiation in Drosophila melanogaster. Genetics 179:455–473.
435 Weiss, C. V., J. I. Roop, R. K. Hackley, J. N. Chuong, I. V. Grigoriev, A. P. Arkin, J. M.
436 Skerker, and R. B. Brem. 2018. Genetic dissection of interspecific differences in
437 yeast thermotolerance. Nat Genet 50:1501–1504.

438 Williams, K. M., P. Liu, and J. C. Fay. 2015. Evolution of ecological dominance of yeast
439 species in high-sugar environments. Evolution 69:2079–2093.
440 Winzeler, E. A., D. D. Shoemaker, A. Astromoff, H. Liang, K. Anderson, B. Andre, R.
441 Bangham, R. Benito, J. D. Boeke, H. Bussey, A. M. Chu, C. Connelly, K. Davis,
442 F. Dietrich, S. W. Dow, M. E. Bakkoury, F. Foury, S. H. Friend, E. Gentalen, G.
443 Giaever, J. H. Hegemann, T. Jones, M. Laub, H. Liao, N. Liebundguth, D. J.
444 Lockhart, A. Lucau-Danila, M. Lussier, N. M'Rabet, P. Menard, M. Mittmann, C.
445 Pai, C. Rebischung, J. L. Revuelta, L. Riles, C. J. Roberts, P. Ross-MacDonald,
446 B. Scherens, M. Snyder, S. Sookhai-Mahadeo, R. K. Storms, S. Véronneau, M.
447 Voet, G. Volckaert, T. R. Ward, R. Wysocki, G. S. Yen, K. Yu, K. Zimmermann,
448 P. Philippsen, M. Johnston, and R. W. Davis. 1999. Functional Characterization
449 of the S. cerevisiae Genome by Gene Deletion and Parallel Analysis. Science
450 285:901–906. American Association for the Advancement of Science.
451 Xie, J., Y. Li, X. Shen, G. Goh, Y. Zhu, J. Cui, L.-F. Wang, Z.-L. Shi, and P. Zhou. 2018.
452 Dampened STING-Dependent Interferon Activation in Bats. Cell Host & Microbe
453 23:297-301.e4.
454

455 **FIGURE LEGENDS**
456
457 **Figure 1. *S. paradoxus* is inviable at high temperature.** Each column reports the
458 viability of a culture of *S. cerevisiae* DBVPG1373 or *S. paradoxus* Z1 at the indicated
459 temperature. The *y*-axis reports the number of viable colony forming units (CFU) per
460 unit of optical density after 24 hours of incubation, as a difference from the analogous
461 quantity at time zero. Each point reports results from one biological replicate, and each
462 bar height reports the average across replicates (n = 3-6). *, P<0.05 for a one-sided
463 Mann-Whitney U test assessing the advantage of *S. cerevisiae* over *S. paradoxus* at a
464 given temperature.
465
466 **Figure 2. *S. paradoxus* alleles of thermotolerance genes confer temperature-**
467 **dependent defects in the *S. cerevisiae* background.** Each panel reports the results
468 of growth experiments of a strain of *S. cerevisiae* DBVPG1373 harboring the indicated
469 gene from *S. paradoxus* Z1, or the respective wild-type parent strains (WT), across a
470 temperature gradient. In a given panel, the *y*-axis reports growth efficiency, the optical
471 density reached by the culture after 24 hours at the temperature indicated on the *x*-axis,
472 as a difference from the analogous quantity at time zero. Each point reports results from
473 one biological replicate (n = 3), and the line represents the average growth efficiency of
474 the indicated strain across the temperature gradient. *, $P < 10^{-3}$ for the strain by
475 temperature interaction term of a two-factor ANOVA, in a comparison between the
476 indicated strain and wild-type *S. cerevisiae*.
477
478 **Figure 3. Thermotolerance genes are enriched for low Tajima's D in *S. cerevisiae*.**
479 The *x*-axis reports the median Tajima's D across a gene set of interest in genomes of
480 wine/European strains of *S. cerevisiae* from (Peter et al. 2018). Blue bars reflect the
481 results from genomic resampling, with the *y*-axis reporting the number of randomly
482 chosen gene sets with the median Tajima's D shown on the *x*, and the blue curve
483 showing a kernel density estimate of the histogram bar values. The red vertical line
484 reports the Tajima's D value of the four thermotolerance genes characterized in Figure
485 2, corresponding to resampling P = 0.0263.

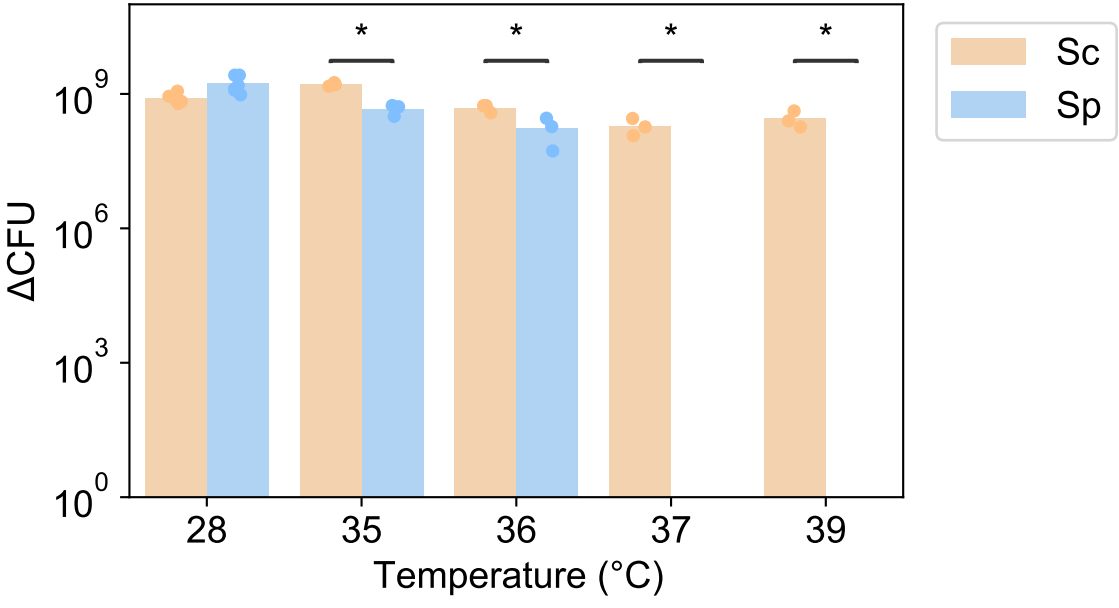
*
*
*
*
Sc
Sp
10^9
10^6
10^3
10^0
ΔCFU
28
35
36
37
39
Temperature (°C)

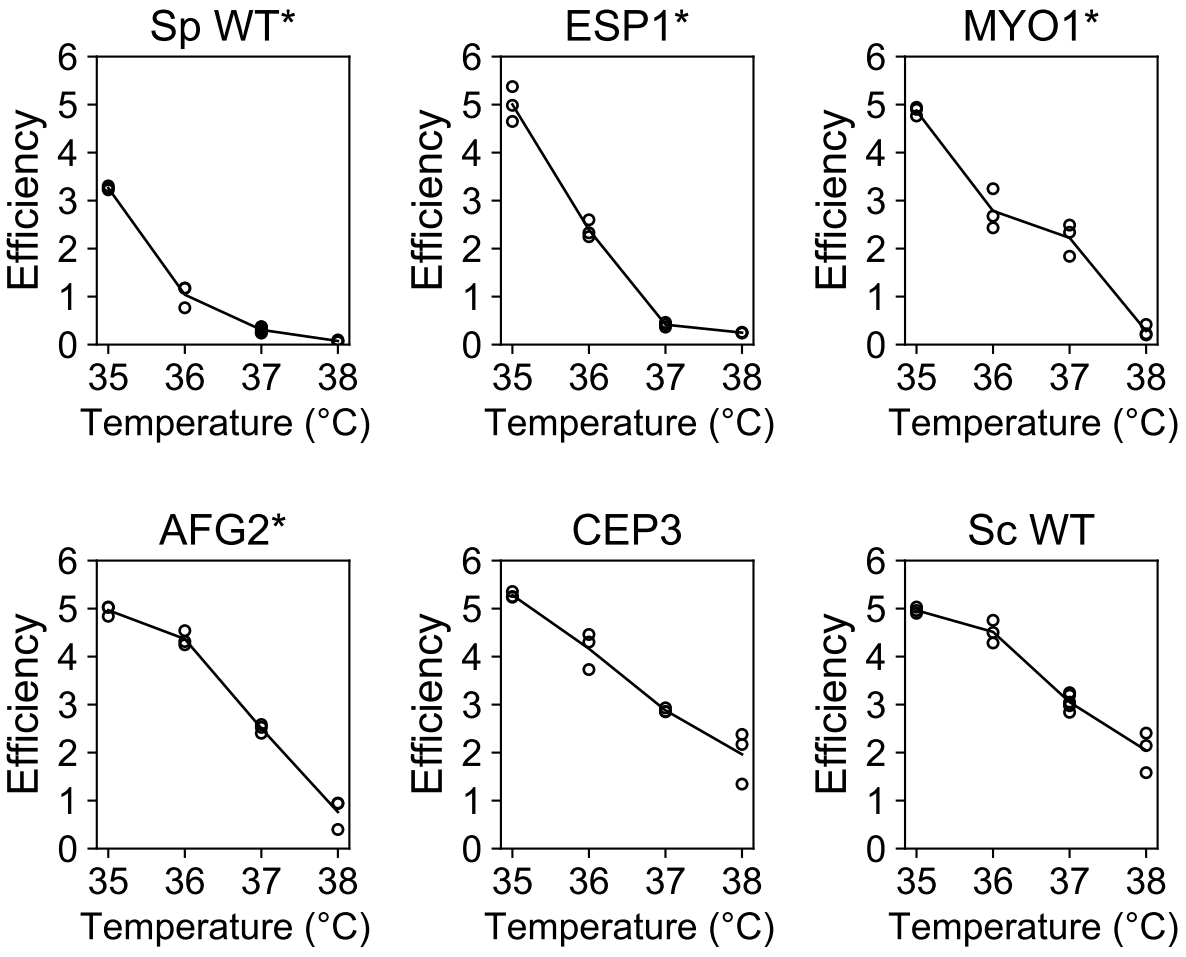
Sp WT*
ESP1*
MYO1*
AFG2*
CEP3
Sc WT
Efficiency
Temperature (°C)
0
1
2
3
4
5
6
35
36
37
38

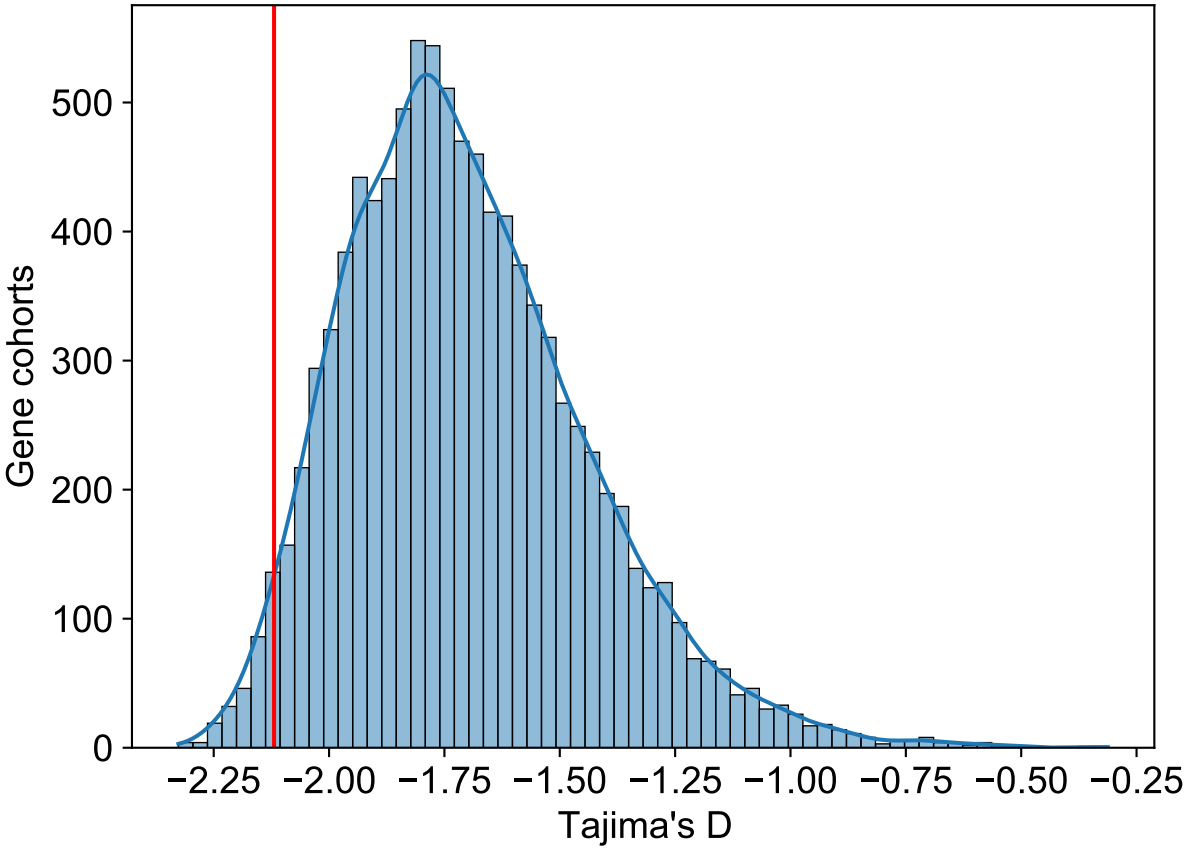
Gene cohorts
0
100
200
300
400
500
−2.25
−2.00
−1.75
−1.50
−1.25
−1.00
−0.75
−0.50
−0.25
Tajima's D